Acta Chemica Scandinavica, 1998: 52: 391–398
Printed in UK – all rights reserved

ACTA
CHEMICA SCANDINAVICA
ISSN 0904–213X

The Analogy Between C=O and C=C(CN)$_2$: Structural Properties of 3-(*N,N*-Dialkylamino)propenones and 4-(*N,N*-Dialkylamino)-1,1-dicyano-1,3-butadienes

Hege Karlsen, Per Kolsaker,* Christian Rømming and Einar Uggerud

Department of Chemistry, University of Oslo, PO Box 1033 Blindern, 0315 Oslo, Norway

Dedicated to Professor Lennart Eberson on the occasion of his 65th birthday

Karlsen, H., Kolsaker, P., Rømming, C. and Uggerud, E., 1998. The Analogy Between C=O and C=C(CN)$_2$: Structural Properties of 3-(*N,N*-Dialkylamino)propenones and 4-(*N,N*-Dialkylamino)-1,1-dicyano-1,3-butadienes. – Acta Chem. Scand. 52: 391–398. © Acta Chemica Scandinavica 1998.

The barriers to rotation around the carbon–amino nitrogen bond in (3-(*N,N*-dimethylamino)-1-phenyl-2-propenylidene)propanedinitrile (**1a**), (3-*N,N*-diethylamino)-1-phenyl-2-propenylidene)propanedinitrile (**1b**), 1-phenyl-[(3-(*N*-pyrrolidine)-2-propenylidene)propanedinitrile (**1c**), 3-(*N,N*-dimethylamino)-1-phenyl-2-propene-1-one (**2a**), 3-(*N,N*-diethylamino)-1-phenyl-2-propene-1-one (**2b**) and 1-phenyl-(3-*N*-pyrrolidine)-2-propene-1-one (**2c**) were determined using ^{1}H NMR spectroscopy. X-Ray crystal structures of **1b**, **1c**, **2b** and **2c** were determined, and quantum chemical calculations were carried out for model compounds of **1** and **2** and for the transition state for the rotation process for these models. The measured barriers (by NMR) for compounds **2** were about 10 kJ mol^{-1} lower than for compounds **1**, results explained by the longer bond distance between the amino nitrogen and the connecting carbon atom in the former compounds, and qualitatively in line with the calculation results. Bond lengths around the C=C(CN)$_2$ structure element indicate that the conjugation in the chain in **1** does not involve the cyano groups, and that their electronic effect is purely electrostatic; they only exert an inductive effect on the conjugated system.

The chemical similarities between compounds carrying an oxygen atom and those where this atom was exchanged with the structural element C(CN)$_2$ (*Die O–C(CN)$_2$-Analogie*) was reviewed in 1976.[1]

Spectroscopically, the carbonyl carbon is highly deshielded. Pertinent to our study, the chemical shift of this carbon in 4-acetylbenzoic acid is ca. 195 ppm,[2] while the analogous carbon in 2-(2,2-dicyano-1-methylethenyl)benzoic acid (Formula 1) is observed close to 170 ppm,[3] notably closer to the carbonyl carbon resonance than to that of a standard alkene carbon atom (123 ppm). The introduction of geminal cyano groups at a double bond imposes a large electronic asymmetry, as demonstrated by ^{13}C NMR spectroscopy; a large chemical shift difference of the two alkene carbon atoms, $\Delta\delta \approx 85$ ppm, is observed in the above dicyanoacid.[3] Chemically, the low electron density at the carbonyl carbon-like alkene carbon is demonstrated by its high electrophilicity in Michael reactions.[4]

Recently, we reported on the formation of (3-

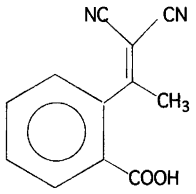

Formula 1. 2-(2,2-Dicyano-1-methylethenyl)benzoic acid.

(*N,N*-dimethylamino)-1-phenyl-2-propenylidene) propanedinitrile (**1a**) in a reaction and particularly on its crystal structure.[5] A high degree of conjugation along the main chain was observed with bond lengths corresponding to a nearly aromatic situation. In ^{1}H NMR spectra of **1a** two well separated methyl signals were observed, similar to the appearance of the methyl groups in the unsaturated *N,N*-dimethylaminoketones **2**.[6] As compounds **2**, where the dicyanocarbon element is replaced with oxygen, can easily be synthezised,[7] it should be of interest to make a comparison of structural and other properties of some analogously substituted compounds **1** and **2** (Formula 2). Thus, dynamic ^{1}H NMR

* To whom correspondence should be addressed.

spectroscopy and single-crystal X-ray structure determinations of these compounds were undertaken together with quantum chemical calculations of some model compounds.

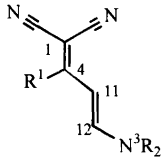

1

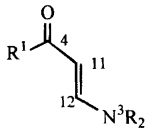

2

Formula 2. Compounds **1** and **2**. **a**, R^1 = phenyl, R = Me; **b**, R^1 = phenyl, R = Et; **c**, R^1 = phenyl, R = R = $(CH_2)_4$; **d**, R^1 = R = H; **e**, R^1 = H, R = Me; **f**, R^1 = phenyl, R = H. Atom numbering according to crystal structures.

Results

Dynamic ^1H NMR. The study by NMR of enaminoketones **2** has focused on two main features, the conformation around the C4–C11 bond and the restricted rotation round the C12–N3 bond. Based on anisotropic effects and electron density calculations on H11 for **2a**–**2c** the conformation around C4–C11 was found to be *syn periplanar*,[8] results also confirmed by our X-ray studies (see below).

Restricted rotation of the C12–N3 bond studied by NMR was first reported in 1963,[6] and has since received considerable attention. The results of our determinations of the barriers to rotation for the various substituted **1** and **2** are entered in Table 1. We found it sufficient for our purpose to use the simplified method of determining the coalescence temperature T_c together with the peak separation at slow exchange ($\Delta\nu$) to estimate the barrier using the well known equation:[9]

$$\Delta G^{\#} = RT_c(23 + \ln T_c/\Delta\nu)$$

The crystal structures. Crystal structure analyses were carried out for **1b**, **1c**, **2a**, **2b** and **2c**. The crystals of **2a** were disordered, and its structure is not reported in the present paper. It was, however, shown to be analogous to those of **2b** and **2c**. ORTEP plots of the four remaining structures are presented in Fig. 1. Some disorder was also present in **1c** where a 30% contribution of another conformer of the five-membered ring is present, the data for which is disregarded in the following discussion. The pertinent structural data are listed in Table 2; for comparison data for **1a** (compound **9** of Ref. 5) are also given. Compound **1c** crystallizes with two molecules in the asymmetric unit (listed as **1cA** and **1cB**, respectively, in Tables 2, 3 and 8). They differ, however, mainly in the torsion angle about the bond connecting the phenyl ring to the main chain. The structures of the series **1** were found to be rather similar, as were those of series **2** compounds. The main differences in the former compounds are found in the dihedral angles between the phenyl and the propanedinitrile moieties, probably caused by the environment in the crystals (cf. Table 3). There are very small differences in corresponding parts in the structures of **2b** and **2c**.

In all the compounds a nearly planar amino group is observed; the deviation of N3 from the plane through C12–C13–C14 being less than 0.04 Å. As may be seen from Table 3 the amino group is nearly coplanar with the plane of the main chain. Since corresponding bond lengths in each of the compound types are equal within 1–3 times the combined estimated standard deviation; we feel that the comparison of the average bond lengths within the propanedinitriles **1** and within the ketones **2**, respectively, is justified.

The conformation around the bond C4–C11 in *syn periplanar* in all substituted **2**, in line with the proposition reported.[8]

Quantum chemical calculation. The results of the calculations are presented in Figs. 2 and 3 and Table 4 (see also Formula 2 for numbering of compounds). Structures **2d** and **2e** are models of the larger compounds **2f** and **2a**, respectively. The latter two compounds differ from the model compounds **2d** and **2e** by having a phenyl group attached to the carbonyl carbon instead of a hydrogen. As evident from the X-ray crystallographic structure of **2b** (the diethyl analogue of **2a**, Fig. 1) the phenyl group is about 27° out of the plane defined by atoms C4, C11 and C12 (Table 3). This leads us to assume that interaction between the π-system of the aromatic ring and the π-conjugated N–C=C–C=O system is of minor importance to the structural and electronic properties of **2f** and **2a**. For this reason we are convinced that **2d** and **2e** will be useful model systems when we later come to discuss the influence of the amino group (and its substitu-

Table 1. Dynamic ^{1}H NMR results of compounds **1** and **2** studied in *N,N*-dimethylformamide-d_7, 0.1 molar solution.

Cpd.	$T_{c(\alpha)}$[a]/K	$\Delta G^{\#}_{(\alpha)}$[a,b]	$\Delta\nu$[c]/Hz	$\nu_{1/2}$[c]/Hz	$T_{c(\beta)}$[a]/K	$\Delta G^{\#}_{(\beta)}$[a,b]	$\Delta\nu$[c]/Hz	$\nu_{1/2}$[c]/Hz	Ref. values[b]
1a	348	73.9±1.0	40.0	2.1					72.1 (DMSO-d_6)[10]
1b	354	75.5±1.0	24.3	2.2	357	75.0±1.0	37.2	1.6	
1c	361	75.7±1.0	38.1	3.3	370	76.9±1.0	49.6	2.2	
2a	312	63.7±1.0	67.5	3.2					63.1 ($CHCl_3$),[8] 60.2 (CH_2Br_2)[11]
2b	282	65.9±1.0	1.7	N.m.[d]	289	64.3±1.0	6.5	2.5	
2c	312	65.6±1.0	91.7	2.7	325	65.4±1.0	33.8	3.0	

[a] α = NCH_3/NCH_2–; β = $-CH_2-/-CH_3$. [b] In kJ mol^{-1}. [c] Δν, peak separation at slow exchange; $\nu_{1/2}$, averaged linewidth at slow exchange. [d] Not measured owing to small Δν.

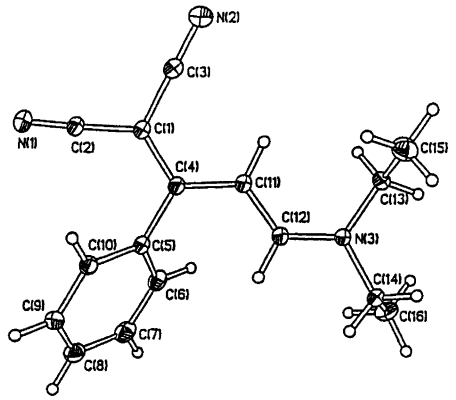

1b

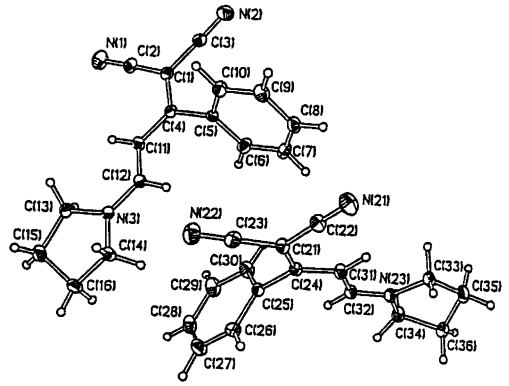

1c

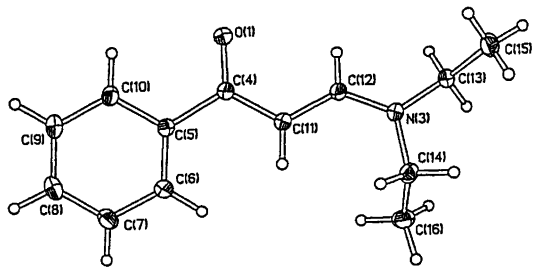

2b

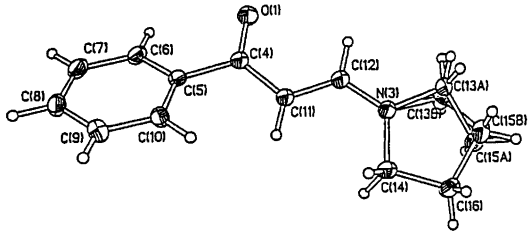

2c

Fig. 1. ORTEP plots of **1b**, **1c**, **2b** and **2c**.

Table 2. Selected structural data.

	1a[5]	**1b**	**1cA**	**1cB**	**2b**	**2c**
Bond lengths/Å						
C4–C5	1.491(2)	1.489(1)	1.494(1)	1.494(1)	1.511(1)	1.507(1)
C1(O1)–C4	1.394(3)	1.405(1)	1.399(1)	1.404(1)	1.245(1)	1.246(1)
C4–C11	1.411(2)	1.410(1)	1.403(1)	1.401(1)	1.434(1)	1.439(1)
C11–C12	1.383(2)	1.391(1)	1.392(2)	1.392(2)	1.381(1)	1.373(1)
C12–N3	1.326(2)	1.328(1)	1.323(1)	1.322(1)	1.334(1)	1.331(1)
N3–C13	1.463(3)	1.468(1)	1.465(1)	1.467(1)	1.468(1)	1.469(1)
N3–C14	1.463(3)	1.473(1)	1.468(1)	1.472(2)	1.465(1)	1.461(1)
Bond angles/°						
C1(O1)–C4–C5	116.9(1)	118.1(1)	117.4(1)	116.3(1)	117.6(1)	118.1(1)
C1(O1)–C4–C11	121.0(2)	120.3(1)	122.1(1)	122.2(1)	123.7(1)	123.6(1)
C5–C4–C11	122.1(2)	121.5(1)	120.4(1)	121.4(1)	118.6(1)	118.3(1)
C4–C11–C12	123.5(2)	123.3(1)	121.9(1)	122.4(1)	119.2(1)	119.6(1)
C11–C12–N3	125.1(2)	125.9(1)	124.2(1)	124.5(1)	127.2(1)	126.2(1)
Torsion angles/°						
C1(O1)–C4–C5–C6	−123.5(2)	127.7(1)	−107.7(1)	−70.3(1)	159.9(1)	23.0(1)
C1(O1)–C4–C11–C12	−177.1(2)	171.7(1)	−173.9(1)	−178.4(1)	−10.6(1)	6.9(1)
C4–C11–C12–N3	−177.8(2)	178.4(1)	177.3(1)	−179.6(1)	176.4(1)	−179.2(1)
C11–C12–N3–C13	−1.0(1)	−2.8(1)	−2.6(2)	0.4(2)	172.2(1)	171.8(1)
C11–C12–N3–C14	175.5(2)	−179.7(1)	−177.1(1)	−178.3(1)	−2.2(1)	0.5(2)

Table 3. Dihedral angles (in °) between nearly planar moieties.[a]

Dihedral angle	1b	1cA	1cB	2b	2c
1–2	55.9	76.9	70.4	26.8	28.9
1–3	55.3	72.1	76.8		
2–3	9.8	7.6	6.4		
2–4	2.4	3.4	1.2	6.8	5.0

[a]Plane 1, phenyl; plane 2, main chain (C4 through N3); plane 3, propanedinitrile group; plane 4, amino group.

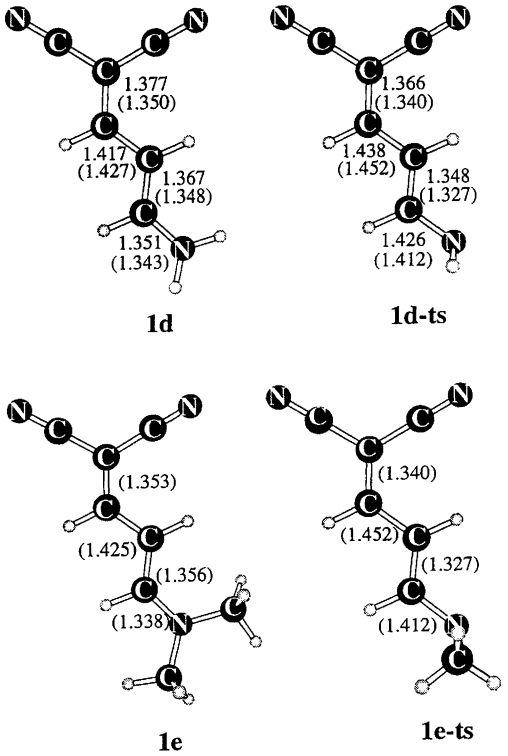

Fig. 2. Bond distances in **1d**, **1e**, **1d**-ts and **1e**-ts derived by quantum chemical calculation (B3LYP/6-31G*, HF/6-31G* values in parentheses).

ents) on these properties. A completely parallel line of arguments can be presented for **1d** and **1e** to be relevant models for **1f** and **1a**. The simplification achieved by omitting the large phenyl group is significant because it allows us to perform reliable quantum chemical calculations which otherwise would be impossible.

The transition structures **2d**-ts and **2e**-ts were obtained for rotation around the C–N bonds of **2d** and **2e**, respectively. Upon rotation of the amino groups several significant changes in the geometries occur. First of all it is clear that the possibility for the nitrogen atom to act as a p-donor is reduced, or even cut off. The bond order of the C–N bond is reduced from partial double bond character in **2d**/**2e** to pure single bond character in **2d**-ts/**2e**-ts. This can be deduced from the increase in the C–N bond lengths. This has immediate consequences for the rest of the chain in that the C=C and C=O bond lengths decrease and the C–C bond length increase. In

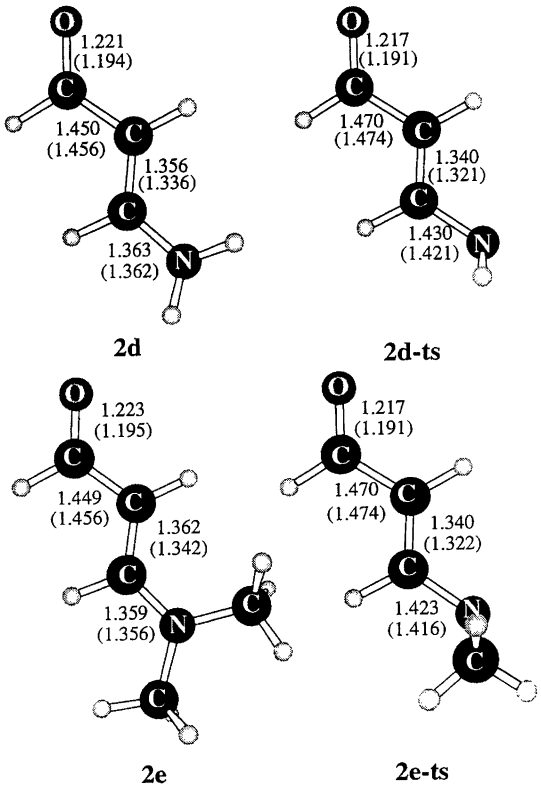

Fig. 3. Bond distances in **2d**, **2e**, **2d**-ts and **2e**-ts derived by quantum chemical calculation (B3LYP/6-31G*, HF/6-31G* values in parentheses).

Table 4. Gibbs free energies (in hartrees, 298 K) from the quantum chemical calculations.

Structure	HF/6-31G*	MP2/6-31G*	B3LYP/6-31G*
2d	−245.742 152	−246.460 909	−247.225 809
2d-ts	−245.727 953	−246.444 973	−247.206 449
2e	−323.743 456	−324.728 885	−325.794 119
2e-ts	−323.729 086	−324.712 457	−325.772 868
1d	−393.348 997	−394.581 087	−395.777 311
1d-ts	−393.331 342	−394.563 700	−395.752 861
1e	−471.350 904	—	—
1e-ts	−471.332 197	—	—

2d/**2e** the nitrogen atom is close to being sp^2-hybridized (the dihedral angles C–C–N–R are below 15 and above −17°, respectively). However, in the transition structure **2d**-ts/**2e**-ts it is sp^3 (the dihedral angles are close to 120 and −120°) with the lone electron pair perpendicular to the π-electron system of C=C–C=O. It should be noticed that another transition structure for rotation around the C–N bond exists. This structure is 4–5 kJ mol^{-1} above **2d**-ts/**2e**-ts and is identical to **2d**-ts/**2e**-ts, except that the C–N is rotated by 180° (stated differently: the configuration on the N atom has been inverted). Because the latter transition structures are of higher potential energy the results have been omitted, and they are not considered to be relevant to the rest of the discussion.

Gibbs free energies for each structure **2d**, **2d**-ts and **2e**,

2e-ts were obtained from the quantum chemical calculations as explained in Experimental section. From these figures the Gibbs free energies of activation for rotation around the C–N bonds of **2d** and **2e** were derived by subtraction (Table 5). The most reliable estimates are expected to come from the B3LYP calculation.

The structural difference between **2e** and **2a** is not believed to be of great significance, as it turns out that only negligible steric interaction between the $-N(CH_3)_2$ moiety and the phenyl group can take place during rotation around the C–N bond.

The effect of replacing the two amino hydrogens in **2d** with the two methyl groups in **2e** on the rotational barrier is rather small judging from the calculations. The methyl groups give barriers which are 10% larger, an effect which we think is due to stabilization of **2e** compared to **2d** by the more polarizable methyl group. In both **2d** and **2e** the nitrogen donates some of its p-electron density into the C=C–C=O group, which makes it more electron deficient. The polarizable methyl group, which may be considered to act as a donor through hyperconjugation, may compensate for some of this deficiency. It is clear that the transition structure is not subject to this stabilization because the nitrogen in that case does no longer act as a p-electron donor.

We will now turn our attention to the model compounds **1d** and **1e** and their corresponding phenyl substituted counterparts **1f** and **1a**. The difference between this series and the one discussed above is that in this series the oxygen atom is substituted by a dicyanomethylene group. It is clear from a comparison between **2d** and **1d** that the degree of conjugation in the C=C–C=C(CN)$_2$ structural element is more pronounced than in C=C–C=O. It is also obvious that the ability of N to act as a p-electron donor increases in going from **2d** to **1d**. This is reflected in the calculated bond lengths (Fig. 2) and barriers of rotation around C–N (Table 5). Owing to the size of **1e** complete geometry optimization could not be performed with MP2/6-31G* or B3LYP/6-31G*.

Discussion

In terms of resonance the reduced rotation around the C12–N3 bond (Fig. 4) is interpreted as high contribution of resonance structure **B** in the description of the resonance hybrid, in MO terms, as results of changes of bond order of the involved bonds, or, in structural terms, as result of changes in bond lengths compared to standard single and double bonds.

Table 5. Gibbs free energies of barriers to rotation ($\Delta G^{\#}$) of model compounds derived from quantum chemical calculations.[a]

Cpd.	B3LYP	MP2/6-31G*	HF/6-31G*
1d	64	46	46
1e	n.c.[b]	n.c.[b]	49
2d	51	42	37
2e	56	43	38

[a] In kJ mol^{-1}. [b] Not calculated, compound too large.

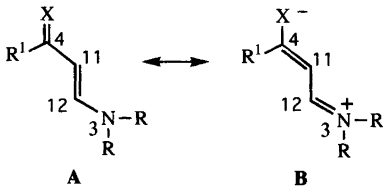

Fig. 4. Resonance structures of **1** [X = C(CN)$_2$] and **2** (X = O).

The measured barriers to rotation in this work (Table 1) are, as expected, in line with the measured bond lengths along the chain X–N3 (Table 2), and qualitatively in line with the quantum chemical calculation (Figs. 2 and 3). Thus, in compounds **1a**,[5] **1b** and **1c**, the formal single bond C4–C11 is $\approx$0.07 Å shorter than a standard C_{sp^2}–C_{sp^2} single bond (1.478 Å),[12] and the formal double bond C11–C12 is $\approx$0.06 Å longer than a standard C_{sp^2}–C_{sp^2} double bond (1.336 Å).[12]

For the compounds **2** the rotation barriers are $\approx$10 kJ mol^{-1} lower, which also is a consequence of the observed bond lengths, as the deviation from the standard values is somewhat smaller (Table 2). The conjugation is apparently less pronounced in the aminoketones. An interesting observation in this connection is that while the deviation from standard bond lengths in C11–C12 is almost the same as for compounds **1** ($\approx$0.05 Å), the C4–C11 bond is only $\approx$0.04 Å shorter than the standard C_{sp^2}–C_{sp^2} single bond. One interpretation seems obvious: the carbonyl oxygen is less effective in taking part in conjugation when compared to the C(CN)$_2$ structural element.

The next question to be asked is: How many atoms are involved in the conjugation in the compounds **1**? Or, in a more scientific way: Does resonance structure **C** (Fig. 5) have a low enough energy to be an important contribution to the real structure of **1**?

For the time being, some of the present authors have been studying the alkylation and acylation of substituted 1,1-dicyanoallylanions, and so far have not been observed any alkylation or acylation at the nitrogen atom.[13] Quantum chemical calculations have been applied in the study of the relative stabilities of acetaldehyde anions and acetonitrile anions leading to the suggestion that the cyano group exerted only inductive stabilization of the latter anion.[14]

A possible answer might be found in the bond distances

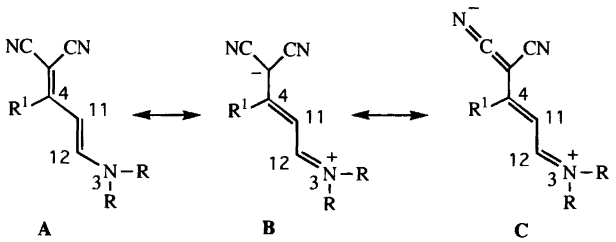

Fig. 5. Resonance structures of **1**.

around the dicyanocarbon structural element in the differently substituted **1** (Table 6). The single bonds to the cyano group seem quite unchanged when compared to the recorded standard values,[12] while the CN triple bond distance is the same as in acetonitrile.[15] A careful conclusion would then be that structure **C** in Fig. 5 has too high an energy to contribute to the structure of **1** and that the effect of the cyano groups is of a purely electrostatic nature, i.e. stabilizing the electron-rich carbon C1 inductively, thus making resonance structure **B** the important one.

A comparison of the geometrical parameters of **2e** (from calculation, B3LYP/6-31G*) with **2b** (from X-ray crystallography) shows that the deviation is 1–2%. The trend towards an increase of the formal double bond distance and a decrease of the formal single bond distance is clear. A similar, but less pronounced, trend is observed in comparison of **1b** with **1e**. Unfortunately, the calculation for the latter compound could only be carried out with a simpler wavefunction (HF/6-31G*).

Regarding the barrier to rotation, in a comparison of the observed and calculated values, two major points must be kept in mind. Firstly, calculated values are strictly valid only for the gas phase, and secondly, for computer time consumption, the phenyl group has been omitted in the model compounds. With these reservations in mind, the calculated values qualitatively show the same trend in that the barrier is lower for compounds **2** by ≈ 10 kJ mol^{-1}, the same difference is also experimentally observed, indicating that conjugation is more pronounced in compounds **1**. The effect of solvation on the barrier heights is manifold in that both the dielectric properties of the solvent as well as specific solvation (e.g. hydrogen bonding) may be operative. It is difficult to estimate how much each of these factors modifies the gas phase (intrinsic) barrier. It has been noted in the literature that there is a general tendency for calculated gas-phase C–N rotational barriers in amides to be slightly lower than the corresponding NMR solution values.[16] From quite extensive measurements on urea and thiourea the authors conclude that it is not likely that the difference in $\Delta G^{\#}$ values predicted by theory and those measured in solution are wholly due to solvent–amide interactions. Unfortunately, a direct comparison of the calculated and experimental numbers in our case is impossible because compound **2a** does not have a sufficient vapour pressure to allow for determination of the NMR coalescence temperature in the gas phase.

The effect of solvents on the measured barrier to rotation for **1a** has been studied, resulting in a general decrease with polarity.[10] A hypothetical extrapolation of the barrier as a function of solvent polarity to gas phase could then lead to values approaching the calculated ones (Table 5).

Experimental

General. Melting points are uncorrected. Infrared spectra were recorded on a Nicolet Magna 550 FTIR spectrometer using an attenuated total reflectance (ATR) ZnSe plate for solid samples. High-resolution NMR spectra (^{1}H and ^{13}C) were recorded on Bruker Spectrospin Avance DPX 200, DPX 300 and DPX 500 spectrometers, ultraviolet spectra on a Shimadzu UV-260 spectrophotometer, and mass spectra were obtained using a Fison Instruments VG ProSpec Q. NMR peak assignments were done using 2D spectroscopy or other suitable pulse programs. All solvents used were dried according to literature recommendations.[17]

Materials.

*(3-*N,N*-Dimethylamino)-1-phenyl-2-propenylidene)propanedinitrile* (**1a**) [m.p. 142–143 °C (acetone–pentane)] was prepared according to a literature procedure.[5]

*(3-*N,N*-Diethylamino)-1-phenyl-2-propenylidene)propanedinitrile* (**1b**) was prepared from (1-phenylethylidene)propanedinitrile and *N,N*-diethylformamide dimethylacetal in 52% yield.[18] M.p. 139.0–139.5 °C (2-propanol). Lit. 134–135.5 °C.[18]

*3-(*N,N*-Dimethylamino)-1-phenyl-2-propene-1-one* (**2a**) was prepared from acetophenone and *N,N*-dimethylformamide dimethylacetal in 67% yield.[6] M.p. 89.5–90.5 °C (chloroform–pentane). Lit. 90–92 °C.[19]

*3-(*N,N*-Diethylamino)-1-phenyl-2-propene-1-one* (**2b**) was prepared accordingly[6] in 33% yield. M.p. 48.5–50.5 °C (diethyl ether/pentane). Lit. 48–50 °C.[19]

*1-Phenyl-[(3-*N*-pyrrolidine)-2-propenylidene]propanedinitrile* (**1c**). To *N*-(4,4-dicyano-3-phenyl-1,3-butadienyl)-*N*,2,2-trimethylpropaneamide[5] (0.5 g, 1.70 mmol) in acetonitrile (5 ml) was added pyrrolidine (0.133 g, 1.90 mmol). After stirring for 15 min acetonitrile was removed, and the crude product was dissolved in dichloromethane and filtered through a short SiO_2 column. Yellow crystals were obtained in 73% yield; m.p. 154–155 °C (chloroform–pentane). IR: ν_{max} 2198 (s,

Table 6. Bond distances in **1** around the dicyanocarbon structural group.[a]

Bond	**1a**[5]	**1b**	**1cA**	**1cB**	Standard values
C1–C2	1.425(2)	1.4247(7)	1.426(2)	1.424(1)	1.427 (sp^2–sp, single)[b]
C1–C3	1.425(3)	1.4246(8)	1.424(2)	1.424(2)	1.427 (sp^2–sp, single)[b]
C2–N1	1.152(2)	1.1609(7)	1.156(2)	1.158(2)	1.1567 (C_{sp}–N_{sp})[c]
C3–N2	1.150(2)	1.1600(9)	1.156(2)	1.155(2)	1.1567 (C_{sp}–N_{sp})[c]

[a]In Å. [b]From Ref. 12. [c]In acetonitrile.[15]

CN), 1598 (s, C=C) cm^{-1}. ^{1}H NMR ($CDCl_3$): δ 7.4–7.3 (3 H, m). 7.2–7.1 (2 H, m), 6.83 (1 H, d, *J* 12.3 Hz), 5.72 (1 H, d, *J* 12.3 Hz), 3.35 (4 H, br m), 2.0–1.8 (4 H, m). ^{13}C NMR ($CDCl_3$): δ 171.0, 152.0, 134.6, 129.5, 128.4, 128.3, 116.8, 116.3, 98.7, 62.4, 53.0, 47.4, 24.6. MS [EI, 70 eV: *m/z* (% rel int.)]: 249 (100, $[M]^{+\cdot}$), 153 (37, $[M-CHCHN(CH_2)_4])^+$. UV [MeOH (log ε)]: λ 393 (4.76), 273 (3.84), 205 (4.12) nm.

*1-Phenyl-(3-*N*-pyrrolidine)-2-propene-1-one* (**2c**). To 3-(*N*,*N*-Dimethylamino)-1-phenyl-2-propene-1-one (**2a**) (0.2 g, 1.14 mmol) dissolved in acetonitrile (5 ml) was added pyrrolidine (0.2 g, 2.8 mmol). After being stirred overnight, the solution was evaporated, and the residue was dissolved in dichloromethane and filtered through a short SiO_2 column. Light yellow crystals were obtained in 64% yield; m.p. 119.5–120.0 °C (choroform–pentane). IR: ν_{max} 1635 (m, C=O), 1582 (m), 1546 (s) cm^{-1}. ^{1}H NMR ($CDCl_3$): δ 7.92 (1 H, d, *J* 12.3 Hz), 7.9–7.8 (2 H, m), 7.4–7.3 (3 H, m), 5.60 (1 H, d, *J* 12.3 Hz), 3.44 (2 H, br s), 3.17 (2 H, br s), 1.90 (2 H, br s), 1.84 (2 H, br s). ^{13}C NMR ($CDCl_3$): δ 188.1, 149.7, 140.4, 130.5, 127.9, 127.3, 92.8, 52.1, 46.8, 24.9. MS [EI, 70 eV: *m/z* (% rel int.)]: 201 (100 $[M]^{+\cdot}$), 184 (19 $[M-OH]^+$, 172 (53 $[M-29]^+$, 105 (31 $[C_6H_5CO]^+$), 70 (30 $[C_4H_8N]^+$. UV [MeOH (log ε)]: λ 347 (4.42), 246 (4.08), 205 (4.18 nm).

NMR measurements. Variable-temperature ^{1}H NMR spectra were obtained using a Bruker Avance DPX 300 spectrometer. The probe temperature was calibrated in a standard way.

X-Ray crystal structure determinations. X-ray data were collected on a Siemens SMART CCD diffractometer[20] using graphite monochromated Mo Kα radiation (λ = 0.710 73 Å). Data collection method: ω-scan, ω-range 0.6°, crystal-to-detector distance 5 cm. Further information is given in Table 7. Data reduction and cell determinations were carried out with the SAINT and XPREP programs.[20] Absorption corrections were applied by the use of the SADABS program.[21] The structures were determined and refined using the SHELXTL program package.[22] The non-hydrogen atoms were refined with

Table 7. Experimental details for the X-ray determination.

	1b	**1c**	**2b**	**2c**
Crystal data				
Compound	$C_{16}H_{17}N_3$	$C_{16}H_{15}N_3$	$C_{13}H_{17}NO$	$C_{13}H_{15}NO$
Formula weight	251.33	249.31	203.28	201.26
Crystal system	Monoclinic	Monoclinic	Monoclinic	Monoclinic
Space group	*C*2/*c*	$P2_1/c$	$P2_1/n$	$P2_1/c$
a/Å	21.242(1)	19.876(1)	6.272(1)	10.776(1)
b/Å	10.485(1)	9.914(1)	19.204(1)	10.257(1)
c/Å	16.214(1)	13.8064(1)	9.617(1)	9.987(1)
β/°	128.75(1)	90.33(1)	90.11(1)	101.33(1)
Volume/Å^3	2816.3(1)	2720.6(1)	1158.37(5)	1081.85(4)
Z	8	8	4	4
F(000)	1072	1056	440	432
D_x/Mg m^{-3}	1.185	1.217	1.166	1.236
μ(MoKα)/mm^{-1}	0.072	0.074	0.073	0.078
T/K	150	150	150	170
Crystal size	0.3 × 0.3 × 0.2	0.4 × 0.3 × 0.3	0.5 × 0.3 × 0.2	0.4 × 0.35 × 0.2
Data collection				
No. of meas. refl.	22 840	42 307	19 386	16 460
No. of indep. refl.	8171	15 728	6831	5763
No. of obs. ($I<2\sigma I$)	7191	8847	5127	4373
R_{int}	0.021	0.053	0.030	0.029
Maximum 2θ/°	80.8	80.8	80.8	77.8
h-Range measured	−38–36	−35–36	−8–11	−16–18
k-Range measured	−19–17	−17–17	−34–34	−17–17
l-Range measured	−23–29	−24–24	−17–17	−17–16
Refinement (Full-matrix least-squares on F^2)				
No. of parameters	240	463	204	214
$R1[F>4\sigma(F)]$	0.044	0.075	0.061	0.059
$2[I>2\sigma(I)]$	0.119	0.160	0.147	0.143
*R*1 (all data)	0.052	0.144	0.088	0.082
*wR*2 (all data)	0.129	0.193	0.164	0.161
Goodness-of-fit	1.078	1.025	1.063	1.082
$\Delta\rho_{max}$/e Å^{-3}	0.48	0.50	0.58	0.40
$\Delta\rho_{min}$/e Å^{-3}	−0.28	−0.28	−0.21	−0.21

anisotropic thermal parameters; hydrogen positions were calculated from geometrical criteria and refined isotropically. Final figures of merit are included in Table 7.

Positional and equivalent isotropic thermal parameters for non-hydrogen atoms, structure factors, lists of anisotropic thermal parameters, hydrogen parameters, and a complete list of bond lengths, bond angles and torsion angles may be obtained from C.R. upon request.

Theoretical methods. The program system GAUSSIAN 94[23] was used for the calculations. The molecular geometries of all species were first optimized using the 3-21G basis set[24] with the Hartree–Fock method[25] (HF/3-21G). Further refinement was obtained by performing complete geometry optimization using each of the following three wavefunctions/functionals: (i) Hartree–Fock theory with the 6-31G(d) basis set[26] (HF/6-31G*), (ii) Møller–Plesset perturbation theory[27] to second order with the 6-31G(d) basis set (MP2/6-31G*), and (iii) a hybrid density functional theory method according to Becke[28] incorporating the 6-31G(d) basis set (B3LYP/6-31G*). A combination of the Newton algorithm and normal coordinate following algorithms were used for all geometry optimizations. The optimized structures were checked for the correct number of negative eigenvalues of the Hessian (the second-derivative matrix). Analytical force constants were computed at this stage, and the vibrational frequencies were obtained together with the rotational constants. These molecular parameters were used within the framework of the rigid-rotor/harmonic-oscillator approximation to calculate the absolute Gibbs free energies at room temperature.

Acknowledgements. C.R. is grateful to Norwegian Research Council for financial support.

References

1. Wallenfels, K., Friedrich, K., Rieser, J., Ertel, W. and Thieme, H. K. *Angew. Chem 88* (1976) 311.
2. Pouchert, C. J. and Behnke, J., Eds., *The Aldrich Library of ^{13}C and ^{1}H FT NMR Spectra*, Vol. 2, p. 1087B, Aldrich Chem. Co., 1993.
3. Rømming, C., Kolsaker, P., Wiberg, A. and Skjetne, T. *Acta Chem. Scand. 50* (1996) 48.
4. March, J. *Advanced Organic Chemistry, Reaction, Mechanism and Structure*, 4th Edn., John Wiley, New York 1993, p. 795.
5. Kolsaker, P., Karlsen, H. and Rømming, C. *Acta Chem. Scand. 55* (1996) 623.
6. Kramer, H. E. A. and Gompper, R. *Z. Phys. Chem., Neue Folge 43* (1964) 292.
7. Paradkar, V. M., Latham, T. B. and Krishnaswami, A. *J. Heterocycle. Chem. 30* (1993) 1497.
8. Kashima, C., Aoyama, H., Yamamoto, Y. and Nishio, T. *J. Chem. Soc., Perkin Trans. 2* (1975) 665.
9. Williams, D. H. and Fleming I. *Spectroscopic Methods in Organic Chemistry*, 4th Edn., McGraw-Hill, Maidenhead 1989, p. 103.
10. Michalik, M., Zahn, K., Köckritz, P. and Liebscher, J. *J. Prakt. Chem. 331* (1989) 1.
11. Filleux-Blanchard, M. L., Clesse, F., Bignebat, J. and Marting, G. J. *Tetrahedron Lett. 12* (1969) 981.
12. Allen, F. H., Kennard, O., Watson, D. G., Brammer, L., Orpen, G. and Taylor, R. *J. Chem. Soc., Perkin Trans. 2* (1987) 51.
13. Kolsaker, P. *et al. Unpublished work.*
14. Saunders, W. H. Jr. Abstract, 12th IUPAC Conference on Physical Organic Chemistry, Padova, Italy, August 1994.
15. Demaison, J., Dubrulle, A., Bucher, D., Burie, J. and Typke, V. *J. Mol. Spectrosc. 76* (1979) 1.
16. Haushalter, K. A., Lau, J. and Roberts, J. D. *J. Am. Chem. Soc. 119* (1996) 8891.
17. Reichardt, C. *Solvents and Solvent Effects in Organic Chemistry*, 2nd Edn., VCH, Weinheim 1988, pp. 414–416 and references therein.
18. Köckritz, P., Schmidt, L. and Liebscher, J. *J. Prakt. Chem. 329* (1987) 150.
19. Henning, H. G., Bandlow, M., Jedrych, Y. and Berlinghoff, R. *J. Prakt. Chem. 320* (1978) 945.
20. SMART and SAINT Area-detector Control and Integration Software, Siemens. Analytical X-ray Instruments Inc., Madison, WI.
21. Sheldrick, G. M. (1996). *Personal communication.*
22. Sheldrick, G. M. SHELXTL, Version 5. Siemens Analytical X-ray Instruments Inc., Madison, WI.
23. Frisch, M. J., Trucks, G. W., Schlegel, H. B., Gill, P. M. W., Johnson, B. G., Robb, M. A., Cheeseman, J. R., Keith, T. A., Peterson, G. A., Montgomery, J. A., Raghavachari, K., Al-Laham, M. A., Zakrzewski, V. G., Oritz, J. V., Foresman, J. B., Cioslowski, J., Stefanov, B. B., Nanayakkara, A., Challacombe, M., Peng, C. Y., Ayala, P. Y., Chen, W., Wong, M. W., Andres, J. L., Reploge, E. S., Gomperts, R., Martin, R. L., Fox, D. J., Binkley, J. S., Defrees, D. J., Baker, J., Stewart, J. J. P., Head-Gordon, M., Gonzalez, C. and Pople, J. A. Gaussian Inc., Pittsburgh, PA 1995.
24. Hehre, W. J., Ditchfield, R. and Pople, J. A. *J. Am. Chem. Soc. 56* (1972) 2257.
25. Roothan, C. C. *J. Rev. Mod. Phys. 23* (1951) 69.
26. Hariharan, P. C. and Pople, J. A. *Theor. Chim. Acta 28* (1973) 213.
27. Möller, C. and Plesset, M. S. *Phys. Rev. 46* (1934) 618.
28. Becke, A. D. *J. Chem. Phys. 98* (1993) 5648.

Received April 8, 1997.